Chapter: 3

Materials & methods and Experimental Details

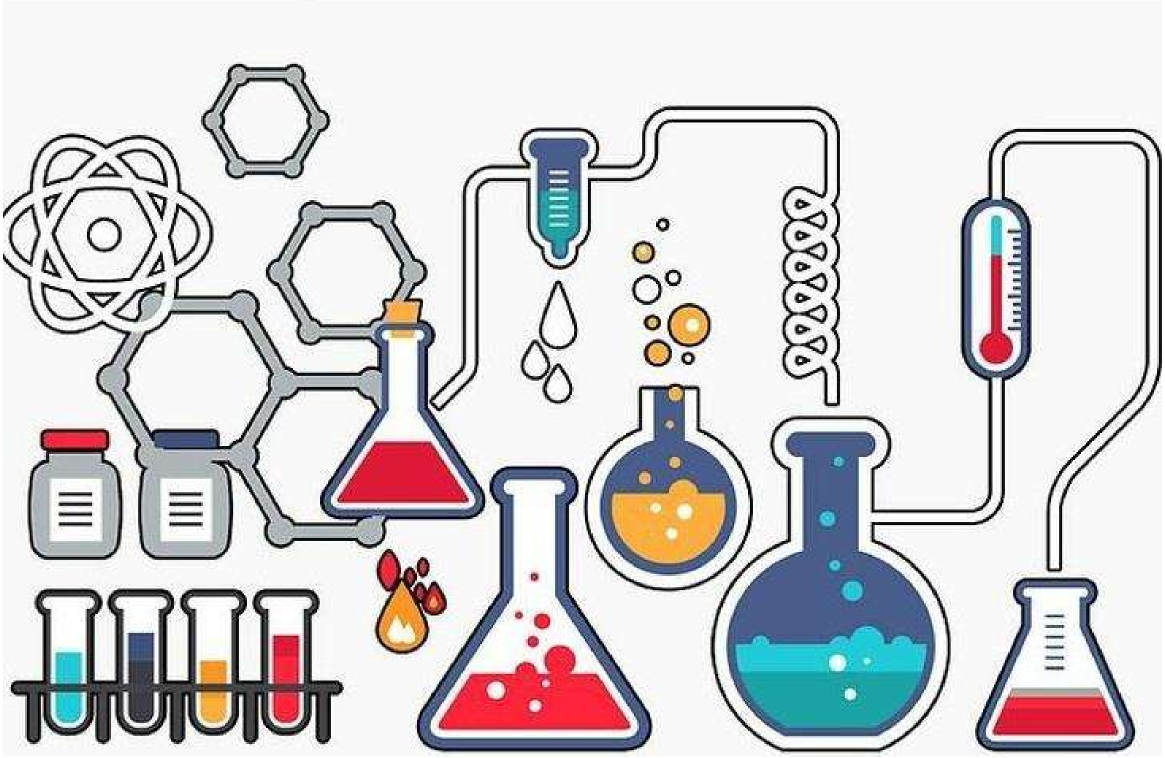

This chapter explains the general methodology for the synthesis of support and mono-metallic catalysts and characterization. This support and catalysts were synthesized by sol-gel, impregnation, and two-step processes and were further calcined in the inert atmosphere to form nano metallic catalysts. In earlier work in our laboratory, Pt/Al_2O_3/La_2O_3/CeO_2 supported catalysts were investigated for oxidative steam reforming of vacuum residue for hydrogen production and found to be an effective catalyst. However, Pt-supported catalysts are not cost-effective for the industrialization of the process. Therefore, in the present study, nickel-based catalysts were investigated for hydrogen production. On the whole, the present study is expected to offer valuable insights into the utilization of MOF-based catalysts for H_2 production through steam reforming of the acetic acid as a model compound of bio-oil. The specific details of materials, methodology for a particular support and catalysts have been explained in this chapter.

3.1 Materials and Methods

Aluminum nitrate nonahydrate ($Al(NO_3)_3{\cdot}9H_2O$, >98%, Merk Pvt Ltd.), Ammonium hydroxide (NH_4OH, >98% Fisher Scientific), Nickel chloride hexahydrate ($NiCl_2 \cdot 6H_2O$,> 98%, Fisher Scientific), Nickel (II) formate ($Ni(HCO_2)_2{\cdot}2H_2O$, >98% Alfa Aesar), lanthanum nitrate ($La(NO_3)_3{\cdot}6H_2O$, >98%, Central Drug House, Mumbai-India), Cerium(IV) sulfate tetrahydrate ($Ce(SO_4)_2 \cdot 4H_2O$, >98%, Merk Pvt.Ltd.), 2'2' Bipyridine ($C_{10}H_8N_2$, >98%, Alfa Aesar), Propan -2OL ($(CH_3)_2{\cdot}CHOH$, >98%, Fisher Scientific), Diethyl Ether ($(C_2H_5)_2O$, >98%, Fisher Scientific), and Ethanol (C_2H_6O, >98% Fisher Scientific) were used directly for the synthesis of support and catalysts.

3.1.1 Preparation of Al_2O_3/La_2O_3/CeO_2 (ALC) support material

High surface area aluminum hydroxide gel was prepared at 30 ºC from a concentrated aluminum nitrate solution by adding ammonia solution. The final pH of the mixture was 9. The prepared hydrogel was kept 24 h for aging and rinsed properly with double distilled water to remove nitrate ions completely. Eventually, the product was dried in an oven and calcined in the furnace at 110 ºC and 800 ºC, respectively, each for 8 h to get γ -Al_2O_3 support. To obtain 3 wt% La_2O_3 yields in the final support, γ-Al_2O_3 support was impregnated with the required amount of aqueous solution of La $(NO_3)_3.6H_2O$. This concentration of La_2O_3 was chosen because it has been reported to be optimal for stabilizing γ-Al_2O_3 support against the sintering process[271] [272]. The γ-Al_2O_3-La_2O_3 support solution was dried on a water bath, further dried in an oven (110 ºC) overnight, and finally calcined at 800 ºC for 8 h. To obtain a 9 wt% concentration of CeO_2 in the final support, the γ-Al_2O_3-La_2O_3 support was impregnated with a required amount of aqueous nitric acid solution Cerium (IV) sulfate tetrahydrate. The obtained mixture was dried in water bath with continuous stirring and subsequently in an oven at 110 ºC for overnight and finally calcined at 600 ºC in presence of air for 8 h. **Fig. 3.1**, shows the general process flow diagram for the synthesis of support.

Preparation of mixed support (Al_2O_3/La_2O_3/CeO_2)

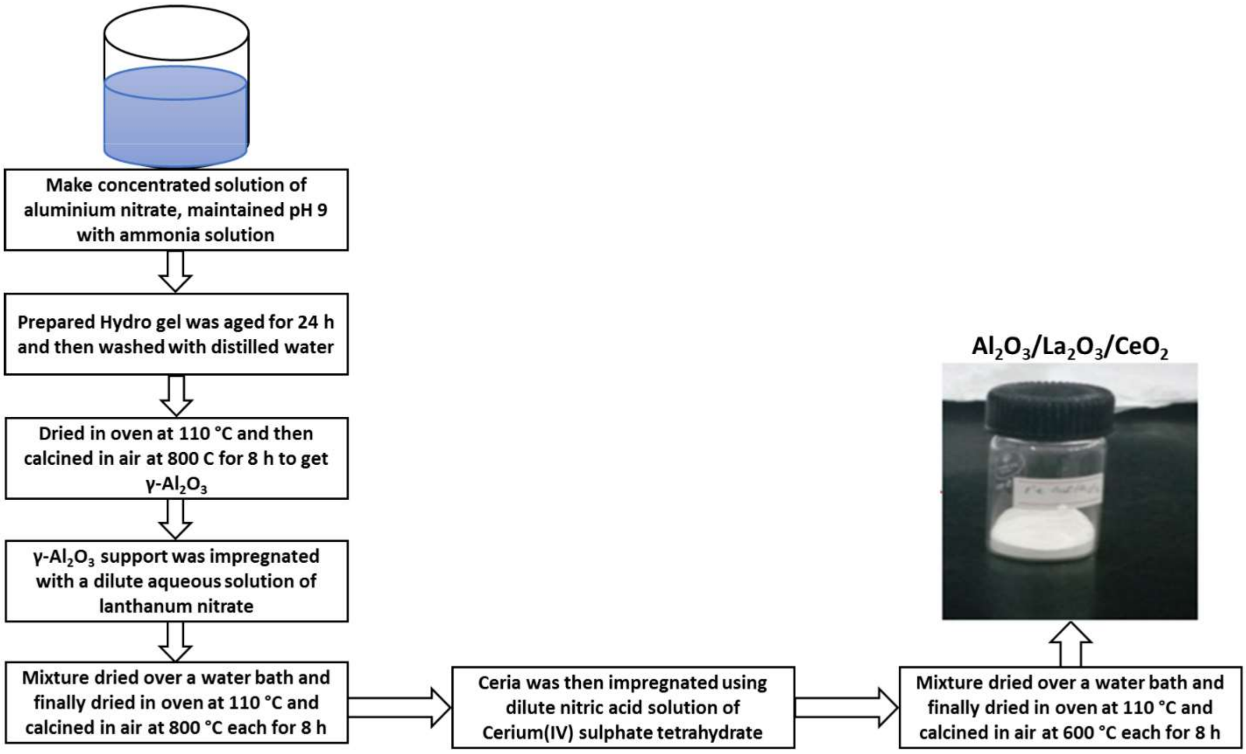

Fig. 3.1. Process flow diagram for the synthesis of support

Synthesis of supported Ni catalyst

The above-synthesized γ-Al_2O_3-La_2O_3-CeO_2 (ALC) support was used to prepare Ni-based catalyst by two different methods. The nickel loading was 15 wt% by weight in both cases.

3.1.2 Synthesis of Ni/ALC catalyst (Catalyst 1)

The catalyst was synthesized by wet impregnation of the support with a dilute ammoniacal nickel formate solution ($Ni(HCO_2)_2.2H_2O$). First, the commercial ammoniacal solution was diluted with water. Then, the requisite volume of the prepared solution was impregnated on the prepared alumina-lanthanum-cerium (ALC) support to obtain 15 wt% Ni in the final catalyst. The obtained mixture was dried in a water bath with continuous stirring and subsequently in an oven at 110 ºC overnight and finally calcined at 650 ºC for 4 h in a tubular reactor in the presence of N_2 flow. The advantage of using nickel formate precursor over other common precursors is that formate does not require external reducing agents like H_2.

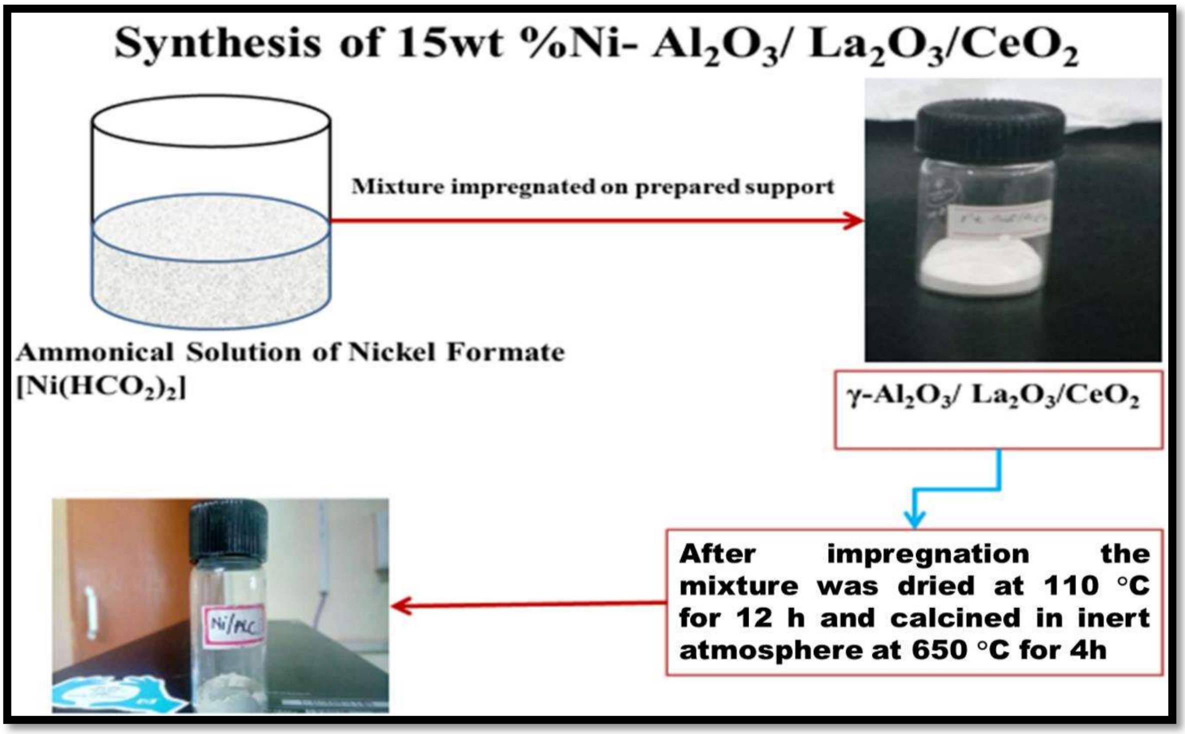

Fig. 3.2. Process Flow diagram for the synthesis of supported catalyst

On heating Ni $(HCOO)_2.2H_2O$ directly decomposes to nickel and a gaseous species [273].

$$\begin{tikzcd}
\mathrm{Ni\ (HCOO)_2.2H_2O} \arrow[r] & \mathrm{Ni\ (HCOO)_2 + 2H_2O} \arrow[d] \\
 & \mathrm{Ni + H_2 + 2CO_2}
\end{tikzcd} \qquad (1)$$

3.1.3 Synthesis of Ni-complex and Ni-complex/ALC catalysts via MOFs then impregnation method

This catalyst was prepared using $Ni[(bipy)_2]Cl_2.6H_2O$ monometallic complex of nickel. A stoichiometric amount of nickel precursor ($NiCl_2.6H_2O$) and organic ligand (2'2' bipyridine) was taken for the preparation of the nano-metallic complexes via the below-given reaction Eq (8). **Fig. 3.3** shows the process flow diagram for the synthesis of the monometallic Ni-complex.

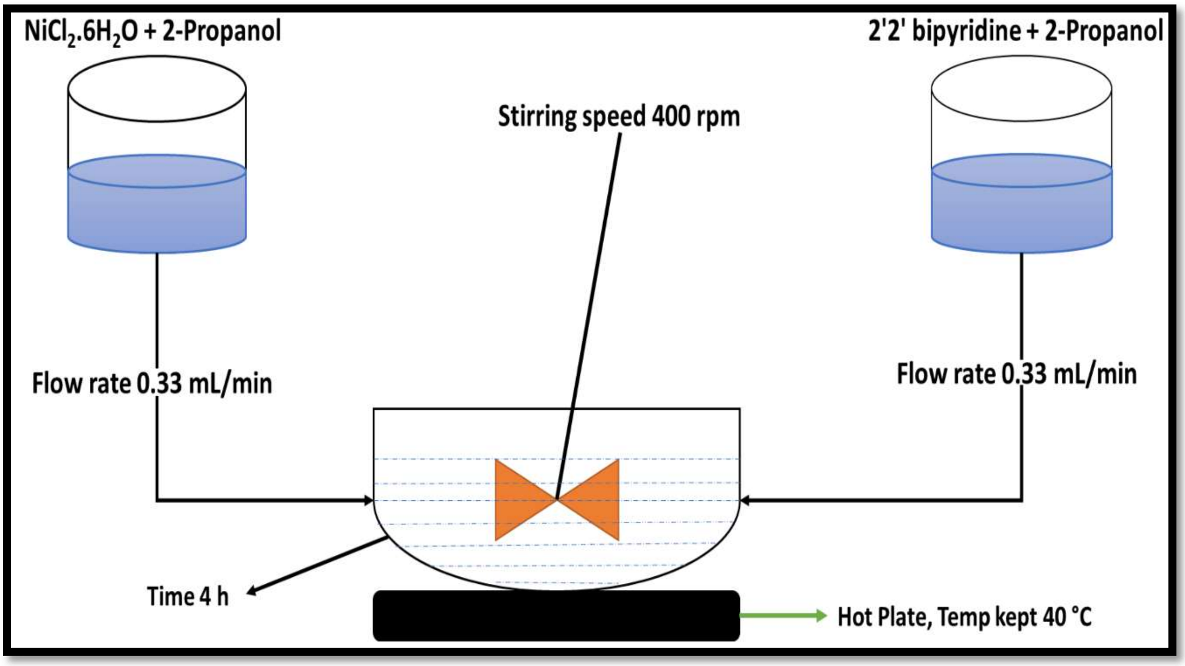

Fig. 3.3. Process Flow diagram for the synthesis of monometallic complex of nickel

$$NiCl_2.6H_2O + 2(bipy) \longrightarrow Ni[(bipy)_2]Cl_2.6H_2O \qquad (8)$$

1.47g of $NiCl_2.6H_2O$ and 3.54 g of 2'2'-bipyridine organic ligand solutions were made in

20 mL of 2-propanol solvent separately. The solutions were mixed dropwise in a round bottom flask simultaneously with continuous stirring at 400 rpm for 4 h. Each solution's flow rate was maintained at 0.33 mL/min, and the temperature of the flask was maintained at 40 °C. The mixture was then filtered and washed with ethanol and ether until free from impurities. Fine pink prism-type crystals, as shown in **Fig. 3.4**, suitable for XRD, were obtained after slow overnight evaporation of mother liquor at room temperature. A molecular structure of $Ni[(bipy)_2]_2.6H_2O$ is made up of $Ni[(bipy)_2]^{2+}$ cationic unit, uncoordinated chloride ions and water molecule of crystallization which are linked through ionic and hydrogen-bonding interaction[274]. The final yield obtained after washing and evaporation overnight was 81% [275].

Fig. 3.4. Ni-complex crystal

The complex was subsequently dissolved in methanol to make a dilute solution for the impregnation of synthesized ALC support. Finally, the solution of the requisite amount of Ni-complex prepared in methanol was taken and mixed with ALC support dropwise in a round bottom flask at 400 rpm, maintaining 40 ºC for 3 h to obtain 10, 15 and 20 wt% loadings of Ni in the final catalysts. The prepared mixture was then washed with ether, dried for 12 h (110 °C) in an oven and calcined for 6 h in the tubular reactor at 650 ºC, the presence of controlled flow N_2 gas to obtain the final catalyst. A process flow diagram Fig. 3.5 and Fig. 3.6 illustrate the synthesis of Ni-complex/ALC catalysts.

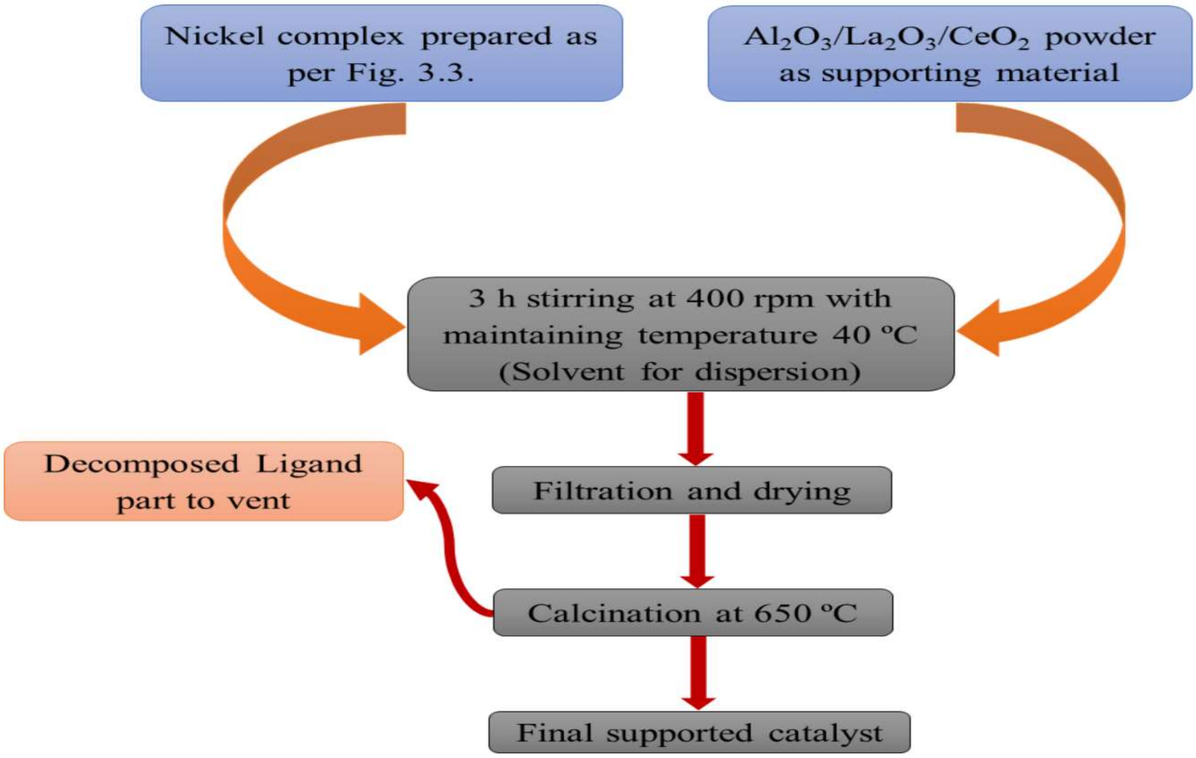

Fig. 3.5. Process flow diagram for supported catalyst

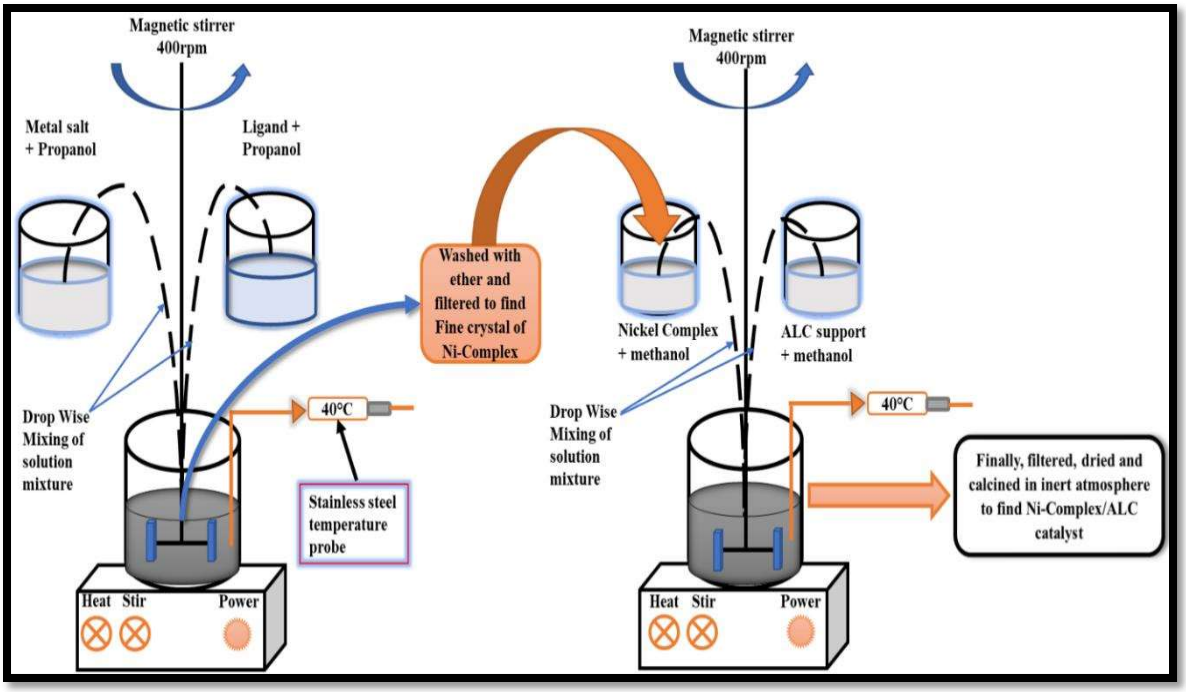

Fig. 3.6. Process flow diagram for the Synthesis of Ni-Complex/ALC

3.1 Table of synthesized catalysts

Sr. No.	Catalyst	Compound	Metal (%)	Preparation method
1.	Support	$Al_2O_3/La_2O_3/CeO_2$ (ALC)	-	Sol-gel and impregnation
2.	Catalyst-1	Ni/ALC	15%	Wet-Impregnation
3.	Catalyst-2	Ni-Complex/ALC	15%	MOFs then Impregnation
4.	Catalyst-3	Ni-Complex/ALC	10%	MOFs then Impregnation
5.	Catalyst-4	Ni-complex/ALC	20%	MOFs then Impregnation

3.2 Experimental set-up for the steam reforming reaction

AASR was studied in a vertical quartz tubular reactor under steady-state conditions **Fig. 3.7** and **3.8** show the details of the experimental set-up. The set-up comprised of three main sections:

(1) Feed entering section:

(2) Reactor

(3) Product analysis section

3.2.1. Feed section

The inlet feed mixture is comprised of nitrogen, water vapor and acetic acid. Water and acetic acid mixture were fed through a calibrated pump (Fluid metric Inc, USA, Model RHSY) at desired flow rates while nitrogen was supplied through a pressurized tank, and its flow rate was controlled via two needle valves fitted in series. The flow of gas was measured and calibrated through a soap bubble meter mL/min. It was possible to control the flow to the accuracy of 0.2 mL/ min at a 10 mL/ min flow rate. Double distilled water was used in all the experiments. At a calculated rate, the mixture of water and acetic acid first entered a pre-vaporizer, kept at a temperature of 150 ºC approximately. Then, the premixed liquid mixture was fed with the desired rate (mL/h) through the calibrated pump (Fluid Metering Inc, USA, Model RHSY). Nitrogen as a carrier gas was also introduced into the reactor at a 30 mL/min flow rate. The pre-heating section consisted of a tubular reactor (inner diameter 5mm and length 400mm) surrounded by the heating coil and insulated with ceramic wools. The temperatures of the pre-heating section were controlled by two variacs connected in series. Nitrogen also entered the pre-vaporizer and swept away steam generated to the top section of the reactor.

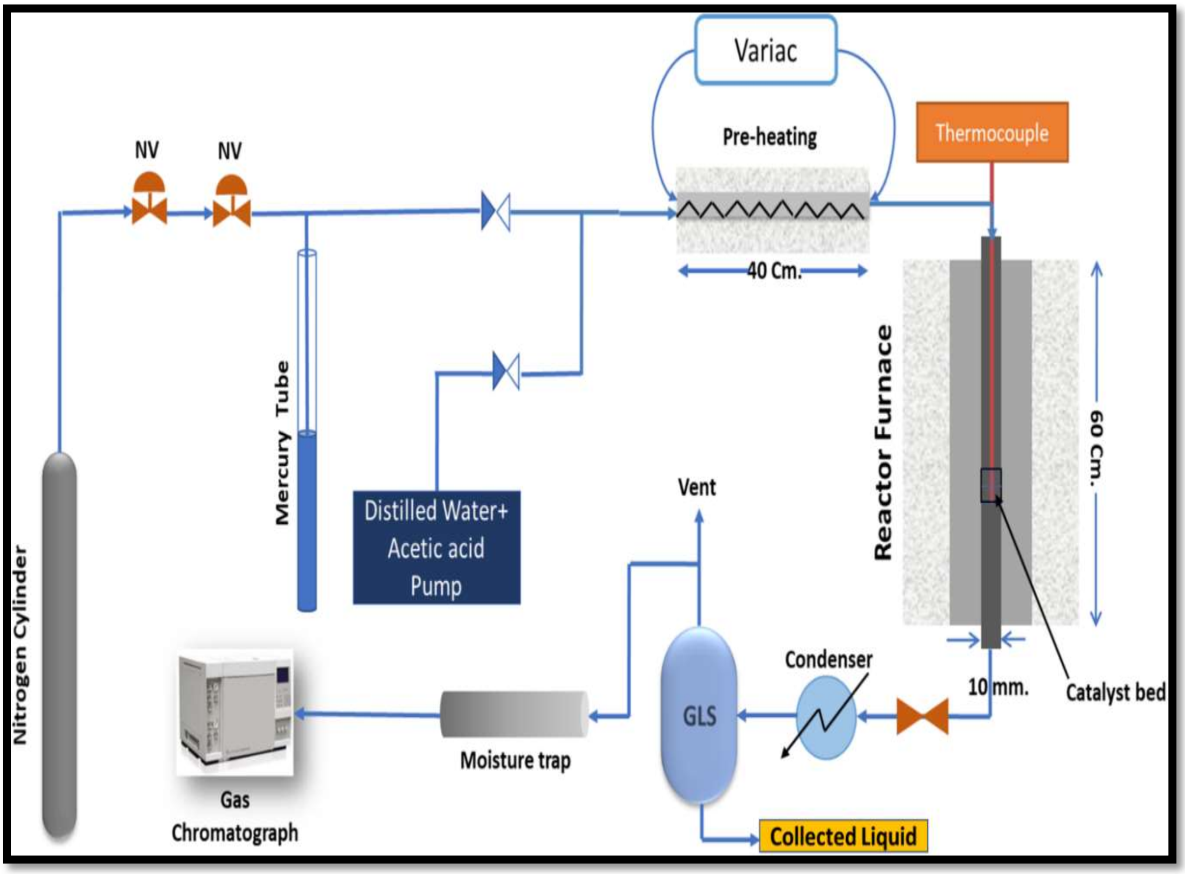

Fig. 3.7. Schematic diagram of the experimental set-up

The mixture of water and acetic acid also entered the top of the reactor. The entire mixture (steam + acetic acid + nitrogen) was then allowed to enter the reactor. A mercury seal with mercury was also provided in the connecting line to avoid any pressure build-up in the system.

3.2.2 Reactor section

The quartz tubular reactor was kept inside a tubular electric furnace with a PID controller (Thermolyne, USA 79300). Fixed bed continuous reactors, either differential or integral, are rated as good as any other type and provide low contact times. This might become an advantage for fast irreversible reactions. The catalytic reactor used in the present study was made of 10 mm inner diameter quartz tube. The reactor was 60 cm long. A K-type thermocouple was placed inside a vertical thermowell at the center of reactor to measure the catalyst temperature. Activity test was carried out using the synthesized catalyst diluted with SiC particles (1:2w/w) (Particles size were of the range of 0.2 - 0.5 mm) to avoid channeling flow and local heating of the catalyst. No catalytic activity was found solely on SiC particles, even at high reaction temperatures. The catalyst particles were placed in the center of the reactor, sandwiched between quartz wool. Thus, the thermocouple could move from the top to the bottom of the reactor. 500 mg of catalyst diluted with SiC, as discussed above, was placed in the central part of the reactor where the temperature variation along the length from the top to bottom of the catalyst bed was not more than 2 ºC. The feed was a mixture of acetic acid and water. Details of the reactor are shown in **Fig. 3.7**. Standard cone and socket joints were used for joining parts of the reactor, the ratio of length and diameter (L/D) should exceed 30 to provide the best conditions for the heat management, and reduction of pressure drop and the ratio of the reactor to catalyst diameters (D/d_p) should be around 6, because of lower dispersion in the axial direction; i.e., along the z-axis. Both the conditions were adequately satisfied in the present study.

Fig. 3.8. A real-time experimental figure

The reactor was mounted vertically, and the reactor bottom section was connected with a gas-liquid separator and helical condenser tube equipped with a cold water bath circulator. The unreacted water and acetic acid were condensed in a gas-liquid separator bypassing the product mixture through a chilled condenser set at 4 °C. The gaseous water vapor in the gas stream was trapped by a moisture trap tube filled with silica gel fine particles.

3.2.3 Product analysis

The gaseous products and condensate liquid were analyzed by Nucon (5700) make gas chromatograph (GC). H_2, N_2, CO, CH_4, and CO_2 in the gaseous mixture were analyzed by a GC-equipped TCD (GC-TCD) with the Carbosieve SII column and the condensate liquid was analyzed by (GC-FID) equipped with Porapak Q column (2m× 1/8′′× 2.2mm). Argon gas was used as the carrier gas. The flow rate of carrier gas was set at 40 mL.min^{-1}. Standard gas mixtures of known compositions (Chemtron Science Laboratory, Navi Mumbai) and liquid standard self-prepared with iso-octane as the internal standard were used for calibration. All the experiments related to conversion, yield and stability tests of catalyst were performed at least twice for the same operating conditions; the experimental data produced were approximately the same with a marginal difference.

The catalyst activity was measured in terms of conversion of acetic acid and yields of species (CO, CH_4, CO_2 and H_2). Conversion of acetic acid was defined in terms of C-C bond cleavage conversion as given below-

Conversion of acetic acid, X_{AcOH} (%)

C-C bond cleavage conversion, $X_{C\text{-}C}$ (%)

$$= \frac{\text{Moles of carbon in the product gases}}{2\times moles\ of\ acetic\ acid\ fed} \times 100 \tag{9}$$

Yields of a species in the products are given in **Eq. (10)** is the ratio of moles of the product species for two times moles of acetic acid fed. On complete conversion of 1-mole acetic acid, 2 moles of CO_2 and 4 moles of H_2 are produced.

The yield of CO, CH_4, CO_2 (%)

$$Y_{\text{CO, CH4, CO2}} = \frac{\text{moles of CO/ CH4/ CO2 out}}{2\times moles\ of\ acetic\ acid\ fed} \times 100 \tag{10}$$

The yield of H_2 produced was calculated using **Eq. (11).** It is the fraction of H_2 produced to the moles of H_2 on complete conversion of 1-mol acetic acid to H_2.

$$Y_{H2} = \frac{\text{moles of H2 production}}{4\times\text{moles of acetic acid fed}} \times 100 \tag{11}$$

3.3 Characterization of catalysts

Structural information of catalysts is essential to understand, explore the relationship between the performance of the catalysts and their microstructure and their preparation techniques. In the present study, appropriate characterization techniques were applied, as given in Table 3.2.

Table 3.2: Characterization techniques used in the present study

S. No.	Characterization technique	Characteristics studied
1	X-ray diffraction (XRD)	Crystal structure - Phase identification and crystallite size
2	Transmission electron microscope (TEM)	Imaging and particle size
3	Selected area diffraction pattern (SAED)	Crystal structure
4	X-ray photoelectron spectroscopy (XPS)	Surface analysis
5	Temperature programmed reduction	reduction behavior and metal support interaction
6	DT-TGA	Decomposition behavior/ Study carbon deposition
7	SEM/EDAX	Textural properties, composition and morphology
8.	Low-temperature N_2 adsorption and desorption	Surface area & pore size distribution

3.3.1 X-Ray diffraction (XRD)

X-ray diffraction technique is used to study the structural information of materials. In this technique, the incident X-rays interact with the specimen and diffracts. Finally, diffracted patterns are collected by occurrence of constructive interference accordingly Bragg's Law:

$$n\lambda = 2d_{hkl}\sin\theta \qquad (3.1)$$

Where n is the order of reflection (any integer), value is taken 1,

λ = wavelength of the incident X-rays

d_{hkl} = the interplanar spacing, and

θ = at which the constructive interference reaches the maximum, i.e., the diffraction angle

Crystalline lattice sizes (D) was calculated from the Scherrer equation:

$$D = \frac{K\lambda}{FWHM\cos\theta} \tag{3.2}$$

Where K = Scherrer constant,

FWHM = full width at half maximum of the reflection peak that has the same maximum intensity in the diffraction pattern,

The Scherrer constant (K) in the formula accounts for the shape of the particle and is generally taken to have the value 0.9.

In the present study, X-ray diffraction patterns of the prepared photocatalysts were obtained from a Rigaku Ultima IV diffractometer using Cu-Kα irradiation. The calculated d-values were matched with standard data for the identification of different phases present in various catalysts. The mean crystallite size of Ni in catalysts was calculated by measuring the line broadening and using the Scherrer formula (Eqn. 3.2).

Actual peak broadening arises from three sources:

(a) Instrumental contributions,

(b) Sample contributions,

(c) Strain in the sample

The instrument contribution needs to be "subtracted" from β_{total} by following Eq$_n$. 3.3 to get actual broadening due to sample.

$$\beta total^2 = \beta instrument^2 + \beta sample^2 \tag{3.3}$$

We neglected the broadening due to strain. The instrumental broadening is obtained from the diffraction pattern of a "standard sample," which consists of large crystallites. In our case standard sample was 'Si,' and the value of broadening due to the instrument was 0.79.

3.3.2 Transmission electron microscope (TEM) and selected area electron diffraction (SAED)

Transmission electron microscopy was used to image and analyze the microstructure of the photocatalytic materials. Measurements were performed in a Tecnai G^2 20 make

TEM at 200 kV accelerating voltage. The powder samples were homogeneously dispersed in pure acetone utilizing an ultrasonic bath and then deposited in the copper grid, and the solvent was allowed to evaporate under vacuum before analysis.

Selected area electron diffraction (SAED) uses diffracted electrons to elucidate crystallographic information from selected regions of the sample. This attachment was employed with TEM. The spacings and orientation of the diffraction spots can be interpreted in terms of planar spacings similar to XRD.

3.3.3 X-ray photoelectron spectroscopy (XPS)

XPS is a technique to analyze chemical property of the surface of any material. XPS spectra can be obtained by irradiating a sample with an X-ray beam while simultaneously measuring the kinetic energy and number of electrons that escape from the analyzed sample. Ultra-high vacuum (UHV) condition is required during analysis. Soft X-rays (i.e., MgK_α) are used as a source. The specimen absorbs photons, and then electrons are ejected via the photoelectric effect. The energy of the ejected electrons can be written as:

$$E_{kE} = h\nu - E_{BE} \tag{3.4}$$

Where, E_{kE} is the energy of the ejected electron,

hν is the energy of the incident photon, and

E_{BE} is the energy of the involved bound electron state.

Binding energy is specific for individual elements. Therefore, identification of a particular element will be possible by measuring the photoelectron energy. It should be noted that for multi-component samples, the intensities of the peaks are proportional to the concentration of the element within the sampled region.

In the present study, XPS studies were carried out on AMICUS, Kratos Analytical using monochromated MgKα (1253.6 eV) as an X-ray source. A vacuum of 2×10^{-6} kPa was maintained in the analyzer chamber. A value of 284.6 eV for the carbon C 1s peak was used as calibration for all measurements. Raw peaks were deconvoluted accurately using XPS peaks 4.1 software.

3.3.4 Temperature programmed reduction (TPR)

Temperature-programmed reduction (TPR) analysis is a widely used technique for characterizing metal oxides, mixed metal oxides, and metal oxides dispersed on a support. The TPR analysis yields quantitative information of the reducibility of the oxide's surface and the heterogeneity of the reducible surface.

In the present study hydrogen programmed reduction (H_2-TPR) technique was performed employing (Micromeritics, model AutoChem II 2705) instrument attached with a thermal conductivity detector (TCD). Each time 60 mg of calcined catalyst sample was introduced into a U-shaped quartz reactor, confined between two quartz wool plugs to prevent the samples from being swept away. Catalysts were also pre-oxidized in the same instrument with the constant oxygen flow at 500 °C for 2 h before performing reduction analysis. Before reduction analysis, the fresh oxidized catalyst sample was purged with argon gas at 200 ºC for 1 h and then cooled to ambient temperature. Then, the reduction was carried out with a mixture of 10% H_2/Ar at a heating rate of 5 ºC/min up to 700 ºC. During the reduction, the consumed amount of H_2 was recorded with a TCD.

3.3.5 TGA/DTA

Thermogravimetric analysis is a technique whereby the weight of a substance in an environment heated or cooled at a controlled rate is recorded as a time and temperature function. During heating reactions, a loss of weight of the substance undergoing the reactions occur and this weight loss can be recorded using this technique.

In the present study, thermogravimetric analysis of fresh and used catalysts was carried out using Euro Vector EA-3000 equipment. As a result, the total loss in weight and corresponding heat loss/generation (exothermic/endothermic) was obtained. The analysis was carried out by raising sample temperature from 373 K to 1200 K at a 5 K/min rate in the presence of argon for fresh catalyst and in the presence of oxygen for used catalysts.

3.3.6 SEM/EDAX

Scanning Electron Microscopy (SEM) and Field Emission Scanning Electron Microscope (FESEM) was used to characterize the structural analysis of the synthesized catalysts using (SEM, SEM; EVO/18 Research, ZEISS, Germany) and (FESEM, Novo Nano SEM 450, FEI Company of USA, SEA, PTE, LTD) apparatus. Energy-dispersive X-ray spectroscopy (EDAX), also known as energy dispersive X-ray microanalysis, is an analytical technique used for the elemental analysis of the catalysts coupled with SEM apparatus.

3.3.7 N_2 adsorption and desorption

The surface area, pore size and pore volume of the catalysts were determined from N_2 adsorption/desorption technique using a Micromeritics (make USA) ASAP 2020 surface area and pore size analyzer. In addition, the instrument had a provision for cleaning the sample by keeping the same in an evacuated chamber at elevated temperatures.

In the present study, the samples were evacuated to a pressure of 1×10^{-2} bar at 423 K for 2 h and subsequently at 623 K for 12 h. Samples along with the sample holder were then connected to the analysis port. The sample kept in a sample holder was dipped into a liquid nitrogen bath during analysis. The dead space calibration was carried out using helium gas. The amount of nitrogen gas adsorbed at any fixed desired pressure was recorded when equilibrium was reached. The data were recorded for the pressure range (p/p^o) from 0.001 to 0.995, where p^o is the vapor pressure of nitrogen. For adsorption studies, the pressure was increased in increment till $p/p^o = 0.995$ was reached. A total of 25 data were recorded. Once the final pressure was achieved, desorption was carried out by decreasing pressure.

BET isotherms were recorded to determine surface area, which accounts for multilayer physical adsorption; it was fitted for adsorption between $p/p^o = 0.05$ and 0.35. The cross-section area of the nitrogen molecule was taken 16.2 $Å^2$

For the pore size analysis, the BJH method, based on the lowering of vapor pressure on a curved surface, was used. In addition, the desorption branch of isotherm was selected for pore size analysis.